A Systematic Approach for Airflow Velocity Control Design in Road Tunnels

Jan Šulc

Czech Technical University in Prague, University Centre for Energy Efficient Buildings, Třinecká 1024, 273 43 Buštěhrad, Czech Republic

Czech Technical University in Prague, Faculty of Electrical Engineering, Department of Control Engineering, Karlovo Náměstí 13, 121 35 Prague 2, Czech Republic

Sigurd Skogestad

Department of Chemical Engineering, Norwegian University of Science and Technology (NTNU) Trondheim, Norway

Abstract

This paper introduces a systematic approach to design and tune the airflow velocity control system for use during fire situations in road tunnels. The proposed approach is focused on road tunnels with a complex structure; long tunnels with connected ramps (entrances and exits), where the controller design can be challenging and time consuming. Such tunnels usually have many sections where a fire can be localized, and this makes the control task difficult. Our approach is based on a simplified one-dimensional simulation model of a tunnel, which includes all the important factors influencing the airflow dynamics of a tunnel. The proportional-integral (PI) controllers are tuned based on the Skogestad Internal Model Control (SIMC) method, which requires a simple model for the process dynamics. The case study is the airflow velocity control in the Blanka tunnel complex in Prague, Czech Republic, which is the largest city tunnel in Central Europe. The results of the paper show how to improve the control algorithm in real operation and how to use the proposed systematic approach for future tunnels.

Keywords: PI controller, SIMC, Control structure design, Road tunnel, Airflow velocity

1. Introduction

Airflow velocity control during fire situations in road tunnels is critical for several reasons [1]:

- to provide suitable conditions for evacuation,
- to support rescue and fire-fighting operations,
- to prevent damage to tunnel installations.

Tunnel ventilation designers have learned a lot from fires in road tunnels that occurred at the turn of the century; Mont Blanc Tunnel (39 fatalities), Tauern Road Tunnel (12 fatalities), St. Gotthard Tunnel (11 fatalities) and Gleinalm Tunnel (5 fatalities), and now invest in safety equipment, especially fire ventilation elements [2].

The main aim of the airflow velocity control during fire in road tunnels is to ensure safe smoke propagation, which means to control the longitudinal airflow velocity. In city tunnels, there are often congestion and stop-and-go situations, and in case of fire, there can be blocked vehicles on both sides (upstream and downstream) of the fire source.

If the longitudinal airflow velocity is about 1.2 m/s, the smoke stays under the ceiling of the tunnel in a separate layer from the fresh air, which extends the time for evacuation [3].

In order to support rescue and fire-fighting operations, the desire is to extract all smoke from the tunnel. In such cases, the longitudinal airflow velocity should be higher than the critical velocity in order to avoid smoke propagation against the direction of airflow. The critical velocity depends on many factors, such as heat release rate of fire, cross-section area of the tunnel, slope of the road, etc., and the exact value can be determined based on detailed Computational fluid dynamics (CFD) simulations. Typical values for critical velocity are in the range of 2.2 to 3.5 m/s [1].

How should we control the longitudinal airflow velocity and which is the most suitable control algorithm? In road tunnels, usually several control techniques are used; some algorithms are closed-loop with various logic elements [4] and some of them are feed-forward due to unreliable measurements of airflow velocity [5]. The most recent published paper [6] introduces nonlinear feed-forward control with the feedback model linearization. Results of this paper are demonstrated by its application to an Austrian highway tunnel. PI controllers are used for the vast majority of industrial processes [7]. Derivative action is normally not included, as it usually has a minor effect on performance and requires filtering of the measurement. Most industrial Programmable logic controllers (PLC) have a standard block for implementing the PI controller. Although the PI controller has only two parameters for tuning, it is still difficult to find the proper values of the proportional gain and the integral time constant. Unfortunately, a lot of engineers still use

Email address: jan.sulc.2@cvut.cz (Jan Šulc)

trial error methods, which in many cases result in poor tuning.

There exist several PI design methods. The classical Ziegler-Nichols method is generally rather aggressive and does not have an adjustable tuning factor. Moreover, this method often requires experiments with oscillations, which could have serious consequences for the controlled process. An analytically based method, Internal Model Control (IMC), was introduced by Rivera, et al. [8]. It gives good results for set-point changes, but it does not have a good disturbance response for integrating processes. Skogestad improved this method to get a good response also for integrating processes. This method is known as the SIMC tuning method [9].

The aim of the paper is to propose a simple systematic procedure for how to design and tune the PI controllers for ventilation airflow velocity. The case study is the airflow velocity control system in the Blanka tunnel complex in Prague, Czech Republic. Originally, the PI controllers of the ventilation airflow velocity in the Blanka tunnel complex were tuned using the root locus method based on knowledge of the process dynamics. Nevertheless, it can not be considered as a systematic procedure. In practice the root locus is more ad hoc, because there are many tuning parameters and no simple tuning guidelines. The paper shows how to design the PI controllers for a complex tunnel system using a systematic procedure, the SIMC method, which is probably the best simple tuning method for proportional-integral-derivative (PID) control. The results of the paper are recommendations and suggestions for improvements of existing airflow velocity control system for real operation of the Blanka tunnel complex. The suggested approach can be also used in the future for the design of airflow velocity control system in other complex tunnels.

2. Case study: the Blanka tunnel complex in Prague

2.1. Basic characteristics of the tunnel

The Blanka tunnel complex in Prague forms the north-west part of the Prague City Ring Road and represents the largest road tunnel complex in the Czech Republic. It is a tunnel complex, which means, it consists of three road tunnels; Bubeneč, Dejvice and Brusnice, which are connected together through tunnel crossroads (ramps); see Figure 3. It is a double tube tunnel with unidirectional traffic in each tube and the total length of the tunnel is approximately 5.5 km. The route passes the urban development and partially also the historical center of Prague and the average traffic intensity is about 60000 vehicles per day (altogether in the whole tunnel) [10].

2.2. Fire ventilation system

The fire ventilation system of the Blanka tunnel is longitudinal with transverse extraction of smoke. In most of the tunnel sections, smoke is extracted with controllable dampers (valves, which regulate the airflow inside the duct) and further through fans in ventilation machine rooms and stacks from the tunnel to the outside environment. In sections that are located within, or close to the exit ramps, the smoke is extracted longitudinally. A schematic illustration of smoke extraction in case of fire is depicted in Figure 1.

There are five ventilation machine rooms intended for smoke extraction; Trója, Letná, Špejchar, Střešovice and Prašný most. The ventilation machine rooms are equipped with axial fans with variable speed, see Figure 2.

The longitudinal airflow is controlled by 88 jet fans. The jet fans are located in couples or triplets at the ceiling of the tunnel, see Figure 4. Some of them are equipped with variable speed drives, which allow continuous regulation of speed, however the majority of the jet fans can be controlled only by start/stop (they are equipped with soft-starters). All the jet fans are fully reversible, which means that they can either support airflow velocity in the traffic direction or, if necessary, to brake the airflow velocity.

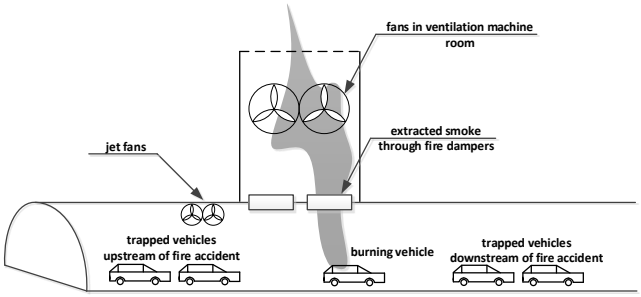

Figure 1: Smoke extraction through controlled dampers and fans in ventilation machine rooms during fire situations.

Figure 2: Ventilation machine room Letná including three axial fans for smoke extraction from the tunnel (2015) [11, 12].

There are three independent sensor systems for fire detection. The primary source for fire detection is a linear heat detector, which is an optical cable that detects increased temperature. The other sensors are smoke detectors and closed-circuit television (CCTV). Together, there are 125 detection sections (marked as SM1-SM125), where a fire can be localized. The length of each section is about 80 m.

After the confirmation of a fire, there are two stages of fire ventilation using the PI controllers of airflow velocity. The ma-

Figure 3: Aerial map of the Blanka tunnel complex in Prague, Czech Republic [11].

Figure 4: A pair of jet fans located at the ceiling of the tunnel. On the left, you can see the entrance ramp Prašný most. The photo was taken during the construction of the tunnel (February 2014) [11].

nipulated variable (u) are the jet fans in the tunnel and the controlled variable (y) is the longitudinal airflow velocity upstream of the fire location. The aim of the first stage, the evacuation stage, is to control the longitudinal airflow velocity, and the set-point value is 0.9-1.6 m/s (depending on the location of the fire). In the second, fire-fighting stage, the set-point value is increased to 1.9-3.6 m/s (critical velocity), in order to avoid smoke propagation against fire-fighters.

The set-point values are determined based on CFD simulations and they depend on cross-sections area of the tunnel and road gradient (declining sections need higher set-point values to avoid smoke propagation against the traffic).

3. A Systematic procedure for airflow controller design

We here describe a systematic procedure for the design of the airflow velocity control system in a road tunnel based on simple PI controllers. The fire ventilation system is activated in the detection section where the fire occurs. In the Blanka tunnel complex, there are 125 detection sections, which means that up to 125 different PI controllers need to be designed. Fortunately, many sections are similar, which reduces it to about 23 controllers. In this paper, we discuss two of these controllers. We do not here discuss the fire detection system (see [13] for details), which activates the appropriate airflow velocity controller.

Consider the feedback control scheme in Fig. 5, where $u(t)$ is the manipulated variable, which consists of $u_1, u_2, \ldots u_i(t)$ the relative speeds of the individual jet fans, and $e(t)[\mathrm{m/s}]$ is the control error for the airflow velocity.

The splitter block defines how each manipulated input u_i is sequenced as the controller output u changes. The splitter block can be based on logic or it could be a split range block.

The controller $c(s)$ is a PI controller

$$c(s) = \frac{u(s)}{e(s)} = K_c \cdot \frac{\tau_I s + 1}{\tau_I s} \tag{1}$$

where K_c is the controller gain (proportional constant) and τ_I is the integral time constant.

With the splitter block, the overall controller is single-input multiple-output (SIMO) as shown in Figure 5.

3.1. Sequence of jet fans (splitter block)

The first design decision is the sequence in which the jet fans u_i should be started (priority list). There will be one sequence for the first stage and an additional sequence for the second stage of fire ventilation. The priority list is defined for every section of the tunnel.

The priority list can be specified according to [1], but it may vary for unidirectional and bidirectional tunnels and short and long tunnels. Moreover, recommendation [1] does not take into account tunnels with connected ramps. The priority list for the Blanka tunnel complex is therefore very specific and is based on the previous experience. The order of jet fans is chosen according to the following criteria:

i) Distance from the fire: Obviously, it makes no sense to start a jet fan located far from the place of the fire, as it has a little effect on the controlled airflow velocity. On the other hand, in order to avoid potential spread of the fire, it is prohibited to start jet fans that are located very close to the fire.

ii) The jet fans equipped with variable speed drive are started before jet fans with soft-starters, since they are more flexible in speed change. Moreover, jet fans equipped with soft-starters have at most 6 starts per hour and there is a minimum time of 6 minutes before each stop and start. On the other hand, jet fans with variable speed drive have no such restriction.

iii) Jet fans located upstream of the fire are started before jet fans located downstream of the fire and jet fans downstream can be used only in the second stage of fire ventilation.

3.2. Detailed distribution of manipulated variable to individual jet fans (splitter block)

The next decision is to decide more precisely on the relationship between the manipulated variable $u(t)$ from the controller and the individual outputs $u_i(t)$ (relative speeds) for each of jet fans. For a section with a single jet fan ($i = 1$), we have $u_1(t) = u(t)$. However, for a system with more than one jet fan, there are many possible choices and many of them are based on logic.

A simple approach, but not optimal, is to distribute the manipulated variable $u(t)$ equally to the jet fans. Assume for now that $u(t) > 0$ and that each individual jet fan operates between $u_i(t) = 0$ (off) and $u_i(t) = 1$ (full speed). With equal distribution, we start up one jet fan at a certain time t, such that we always have

$$\sum_{i=1}^{k} u_i(t) = u(t) \tag{2}$$

For example, for a case with four jet fans ($k = 4$) and for the value $u = 2.4$ of the manipulated variable, we could achieve this with

$$u_1 = 1, \quad u_2 = 1, \quad u_3 = 0.4 \quad \text{and} \quad u_4 = 0.$$

Thus, jet fans 1 and 2 are running at full speed, jet fan 3 is running at 40% and jet fan 4 is off. However, in our case, this does not work, because only the first jet fan in the priority list is generally adjustable, that is, with variable speed drive. The other jet fans only allow the values $u_i(t) = 0$ (off) or $u_i(t) = 1$ (on), because they are equipped with soft-starters. We therefore have to use jet fan 1 to do fractions between integer values. For example, for a case with four jet fans and $u = 2.4$, we use:

$$u_1 = 0.4, \quad u_2 = 1, \quad u_3 = 1, \quad u_4 = 0.$$

Thus, jet fans 2 and 3 are running at full speed, jet fan 1 is running at 40%, and jet fan 4 is off.

In addition, in our case, to avoid overheating of a jet fan by running at too low speed, we are not allowed to operate a jet fan between 0 and 30%, thus limiting the operating range for jet fan 1. Therefore, for u between 2 and 2.3 we get in our case

$$u_1 = 0, \quad u_2 = 1, \quad u_3 = 1, \quad u_4 = 0$$

and for u between 2.3 and 3

$$u_1 = u - 2, \quad u_2 = 1, \quad u_3 = 1, \quad u_4 = 0.$$

The fact that u_1 is partly quantized will lead to oscillations with u_1 cycling between 0 and 0.3 for cases where the steady-state set-point for the output y is such that it corresponds to a steady-state average value for u_1 in the range from 0 to 0.3. If u is negative, corresponding to reverse operation of the jet fans, the same procedure applies.

This technique is simple to implement, however it is not the best way, since the jet fans have different dynamic responses. Jet fans located near to the fire have larger influence than jet fans located far from the fire. Possible improvements would be to assign different weights to every jet fan and omit poor performing jet fans from the priority list.

One possible way is to assign different weights to jet fans according to their gains. The gain represents the steady state airflow velocity when starting the jet fan at full speed. For example, consider two jet fans ($k = 2$) where both are equipped with variable speed drives. The gains of both jet fans are:

$$G_1 = 1, \quad G_2 = 1.5$$

For simplification, consider that $u(t) \geq 0$. The manipulated variable is distributed to individual outputs as follows:

$$u_1(t) = \begin{cases} \min\left(1, \frac{u(t)G_2}{G_1+G_2}\right), & \text{if } \frac{u(t)G_1}{G_1+G_2} \geq 0.3 \\ u(t) - 0.3, & \text{if } \frac{u(t)G_1}{G_1+G_2} < 0.3 \text{ and } u(t) \geq 0.6 \\ u(t), & \text{if } 0.3 \leq u(t) < 0.6 \\ 0, & \text{if } u(t) < 0.3 \end{cases} \tag{3}$$

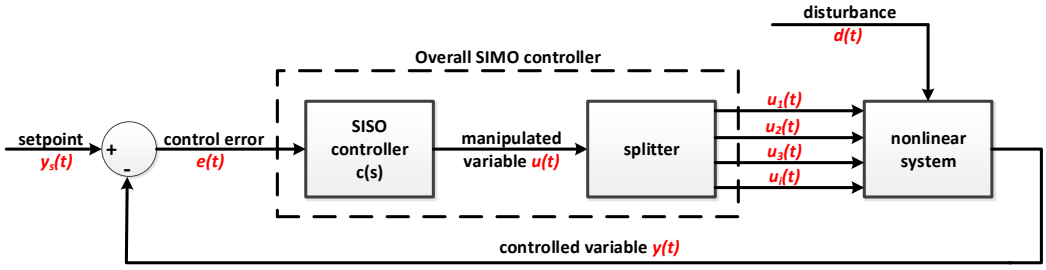

Figure 5: Feedback control loop for the simulation of the airflow velocity control using PI controller; $y(t)$ is the airflow velocity and $u_i(t)$ is the relative speed of the jet fan i.

$$u_2(t) = \begin{cases} u(t) - u_1(t), & \text{if } u(t) \geq 0.6 \\ 0, & \text{otherwise} \end{cases} \quad (4)$$

In Table 1 we show a result of the suggested logic (3, 4) for different $u(t)$.

Table 1: Distribution of manipulated variable $u(t)$ to jet fans u_1 and u_2 according to suggested logic (3, 4).

$u(t)$	$u_1(t)$	$u_2(t)$
0	0	0
0.3	0.3	0
0.5	0.5	0
0.6	0.3	0.3
0.75	0.45	0.3
1	0.6	0.4
1.5	0.9	0.6
1.75	1	0.75
2	1	1

From Table 1 we see that formula (2) holds, u_1 and u_2 run simultaneously for $u(t) > 0.5$ and the logic balances the gain of both jet fans (u_1 runs at higher speed). Similar conditions can be derived for negative $u(t)$ and generalized for more jet fans and jet fans with soft-starters, however they are more complex.

3.3. Requirements on airflow velocity control

There are no strict requirements on the airflow control performance for ventilation of tunnels. The Czech national guideline [14], which is not binding and represents only recommendations, says:

- The airflow velocity should be kept in the range $\pm 0.3\ \mathrm{m/s}$ from the set-point value and this range should be achieved within 3 minutes after the start of airflow velocity control,
- Reversal of flow at blocked vehicles is strictly prohibited,
- Disturbances must be suppressed as fast as possible.

These control requirements apply especially for the first stage of fire ventilation, where it is critical to extend the time for evacuation.

3.4. Systematic procedure for PI controller design

In this section we summarize a systematic procedure for PI control of airflow velocity in road tunnels during fire ventilation. The procedure can be summarized in following four steps:

1. Develop or use the existing nonlinear model of airflow dynamics (Section 4). The model cannot be directly used for the design of PI controllers due to its complexity.
2. Simplify the general nonlinear model obtained from point 1 to a multi-input, single-output (MISO) nonlinear system. The system inputs are the relative speeds of jet fans (u_i), which should be started according to the priority list and the system output is the airflow velocity (y) upstream of the fire location.
3. Tune the PI controllers using the SIMC-rule for all detection sections and for both stages of fire ventilation. This procedure is described in Section 5.1.
4. Validate the designed controllers on the nonlinear model of the airflow dynamics including saturation, limitations and anti wind-up protection. Validate the ability of the controller to suppress disturbances.

3.5. Saturation, anti wind-up protection and physical limitations of jet fans

There are upper and lower saturation limits for the manipulated variable u. The upper limit is essentially given by the total number of jet fans in the priority list and the lower limit, corresponding to the number of jet fans that can operate in reverse mode, is given by the number of jet fans equipped with variable speed drive. For example, with one variable speed drive jet fan and three soft-starter jet fans, we have $u_{min} = -1$ and $u_{max} = 4$.

As mentioned before, there is also another physical limitation for jet fans equipped with variable speed drive. They should not work in that low-speed region. For this reason, it is not allowed to operate with u in the range $(-0.3, 0.3)$.

The wind-up may occur, when we use integral control action and the manipulated variable saturates. The simple clamping method for anti wind-up protection is implemented. This simply stops the integration when the manipulated variable (u) saturates.

4. Mathematical model of airflow dynamics

In this section we introduce a detailed, yet simplified model of the airflow dynamics in road tunnels, which is based on the Bernoulli and continuity equations. This nonlinear model is next used to obtain a linearized first-order plus time delay model, which is suitable for tuning the PI controller via the SIMC method. The mathematical model is described in detail in [13], so here we introduce only the main principles of airflow dynamics in road tunnels.

The following convention is used: A positive sign of the airflow velocity denotes direction identical with the direction of traffic.

4.1. Simplified nonlinear model

First, let us state two simplifying assumptions for the nonlinear model:

i) We assume incompressible flow, that is, the density of air ρ is constant along the whole length of the tunnel and does not depend on time,

ii) We consider a one-dimensional model with lumped parameters, i.e. $\frac{\partial v}{\partial y} = \frac{\partial v}{\partial z} = 0$. Together with assumption i) this implies that the airflow velocity v is constant along each section of the tunnel.

Assumption i) is valid for airflow velocities with Mach numbers considerably lower than 1 [15]. This assumption is fulfilled for road tunnels, where the maximum airflow velocity is typically about 7 m/s, which corresponds to the Mach number less than 0.03.

Assumption ii) says that the airflow velocity in a given section of the tunnel does not depend on the y and z coordinates. We consider it to be a reasonable assumption for the mean airflow velocity in the tunnel. Moreover, this assumption leads to a computationally tractable model.

The road tunnel can be divided into sections with constant geometry, cross-section area, hydraulic diameter, etc. An example is shown in Figure 6. The airflow dynamics in each section is described by the generalized Bernoulli equation.

4.2. Bernoulli equation for unsteady flow

The generalized Bernoulli equation for incompressible and unsteady flow is derived in many references, such as [16], and can be expressed in different ways. For our purpose, we use the form

$$\rho L \frac{\mathrm{d}v}{\mathrm{d}t} = \Delta p \tag{5}$$

where $v[\mathrm{m}\cdot\mathrm{s}^{-1}]$ is the airflow velocity (constant along each section), $a = \frac{\mathrm{d}v}{\mathrm{d}t}[\mathrm{m}\cdot\mathrm{s}^{-2}]$ represents the local acceleration of air, $L[\mathrm{m}]$ is the length of the given section of the tunnel, $\rho[\mathrm{kg}\cdot\mathrm{m}^{-3}]$ is the density of air, and $\Delta p[\mathrm{Pa}]$ denotes the total pressure change in the given section of the tunnel and can be expressed as follows:

$$\Delta p = \Delta p_{loss} + \Delta p_{fire} + \Delta p_{JF} + \Delta p_{pist} \tag{6}$$

Here Δp_{loss} include the pressure loss caused by air friction and local resistances (cross-section area changes, dividing and merging flows, etc.), Δp_{fire} is the pressure loss caused by fire, Δp_{JF} is the pressure change caused by running jet fans and Δp_{pist} denotes pressure change thanks to piston effect of vehicles in the tunnel. Details on the calculation of pressure changes and resistance coefficients can be found in [13].

Generally, the term Δp_{loss} is a quadratic function of airflow velocity and can be calculated as follows

$$\Delta p_{loss} = -\frac{1}{2}\rho\zeta(v, A, L, ...)v^2 \tag{7}$$

where $\zeta[-]$ is the resistance factor, which depends on airflow velocity v and tunnel geometry (length L, cross-section area A, etc.).

The pressure loss imposed by fire (Δp_{fire}) can be accurately estimated using CFD simulations. However, there exist also simple formulas for the fire pressure loss in one dimension based on the buoyancy and expansion of the fire [17]. In our model we use the one-dimensional model developed and experimentally verified by Opstad, et al. [18]. The model can be used only for longitudinally ventilated sections without smoke extraction via ventilation machine rooms. Calculation of this pressure change can be performed in the following way:

$$\Delta p_{fire} = -\frac{vg\alpha\rho}{c}\log\left(\frac{T_m}{T_f}\right) \tag{8}$$

where $T_f[\mathrm{K}]$ is the average gas temperature at the location of fire, $T_m[\mathrm{K}]$ is the mean fire temperature, $g[\mathrm{m}\cdot\mathrm{s}^{-2}]$ is the gravitational acceleration, $\alpha[-]$ is the slope of the road (negative value corresponds to the declining section) and $c[s^{-1}]$ is a constant that depends on the convective heat transfer coefficient, hydraulic diameter and heat capacity of air.

According to [19], the average gas temperature at the location of fire can be calculated as follows:

$$T_f = T_0 + \frac{2}{3}\frac{Q}{\rho A C_p v} \tag{9}$$

where $T_0[\mathrm{K}]$ is the ambient temperature, $C_p[\mathrm{Jkg}^{-1}\mathrm{K}^{-1}]$ is the heat capacity of air, $Q[\mathrm{W}]$ is the heat release rate of the tunnel fire.

The mean fire temperature T_m corresponds to the average temperature at the middle point between the fire source and the downstream exit.

The pressure gain from running the jet fans can be expressed as [20]

$$\Delta p_{JF} = k_1 n_{JF} - k_2 n_{JF}\cdot v \tag{10}$$

where n_{JF} is the number of jet fans running simultaneously in the same place of the tunnel (i.e. $n_{JF} = \pm 0, 1, 2, \ldots$), and k_1, k_2 are constants, which depend on the data for the jet fans. The constants k_1 and k_2 also differ for different location of jet fans.

Formula (10) holds only for an integer number of running jet fans. If a jet fan with the variable speed drive is started, the

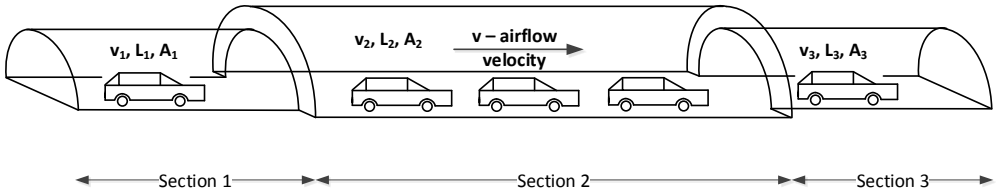

Figure 6: Example of dividing the tunnel into the sections, which have constant parameters; cross-section area, length, hydraulic diameter, slope of the road, etc.

pressure gain depends quadratically on the relative speed of a jet fan

$$\Delta p_{JF} = k_1 \cdot \omega_{JF}|\omega_{JF}| - k_2 \omega_{JF} \cdot v \tag{11}$$

where ω_{JF} is the relative speed of a jet fan with the variable speed drive, i.e. $\omega_{JF} \in \langle 0, 1 \rangle$.

During fire in the tunnel, vehicles located downstream of the fire usually leave the tunnel, but in the case of congestions, there can be blocked vehicles upstream and downstream of the fire. This can be modeled as a disturbance in the nonlinear model.

The stack effect is caused by the temperature differences between portals of the tunnel. A natural buoyancy exists, so air in the tunnel flows from a place with higher temperature into a place with lower temperature. We neglect the stack effect caused by temperature differences at tunnel portals, because in the Blanka tunnel complex, the altitude change of tunnel portals is not significant. However, the stack effect may play a role as a disturbance in our simulation model, thus, it can be used for the testing the robustness of the designed PI controller for airflow velocity control.

We also neglect pressure changes caused by wind at the tunnel portals, because this effect is negligible for the Blanka tunnel complex, thanks to its favorable location in the terrain.

4.3. Bernoulli equations for series-parallel network

The Blanka tunnel complex includes several exit ramps and entrance ramps, see Figure 3, and in this case the Bernoulli equations must be modified to fulfill pressure equality condition at the branches. For example, the tunnel in Figure 7, which is formed by one entrance and one exit tunnel ramp, can be described by the following set of Bernoulli equations

$$\begin{aligned} \rho(L_1 a_1 + L_2 a_2) &= \Delta p_1 + \Delta p_2 \\ \rho(L_2 a_2 - L_3 a_3 + L_4 a_4) &= \Delta p_2 - \Delta p_3 + \Delta p_4 \\ \rho(L_4 a_4 + L_5 a_5) &= \Delta p_4 + \Delta p_5 \end{aligned} \tag{12}$$

where L_i represents the length of the i-th section ($i = 1, 2, 3, 4, 5$), a_i is the local acceleration of air in the i-th section and Δp_i corresponds to the total pressure change in the i-th section of the tunnel.

4.4. Continuity equations for series-parallel network

The continuity equation expresses the conservation of mass, and is sometimes called the mass-balance equation. Under the assumptions stated in section 4.1, the continuity equation for unsteady flows can be written in the following form [21]

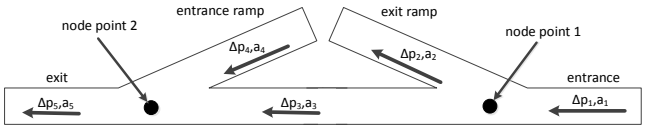

Figure 7: Example of a tunnel complex including one entrance and one exit ramp. Arrows denote traffic direction.

$$\sum_i Q_{v_i} = 0 \tag{13}$$

where $Q_{v_i}[\mathrm{m}^3 \cdot \mathrm{s}^{-1}]$ is the airflow rate in the given section of the tunnel streaming in, respectively out from the node point of the tunnel.

For example in Figure 7, there are two node points resulting in two continuity equations:

$$Q_1 - Q_2 - Q_3 = 0 \tag{14}$$

$$Q_3 + Q_4 - Q_5 = 0 \tag{15}$$

Formula (13) can be rewritten using airflow velocity and cross-section area

$$\sum_i A_i \cdot v_i = 0 \tag{16}$$

The continuity equation applies also for cross-section area changes and extraction of air through ventilation machine rooms.

The final state-space description of the airflow dynamics in a road tunnel complex is based on the set of Bernoulli equations (12) and continuity equations (13), (16).

4.5. State-space description in explicit form

The segmental scheme of the Blanka tunnel complex is illustrated in Figure 8. There are all together 34 state variables, which are the airflow velocities (v_i) in the individual tunnel sections. The system has multiple inputs (u_i), which are the jet fans in the given sections of the tunnel. Further, the system includes the following disturbances: pressure change caused by piston effect of vehicles, pressure loss due to the occurrence of fire, extracted amount of air through ventilation machine rooms, stack effect and wind effect at tunnel portals.

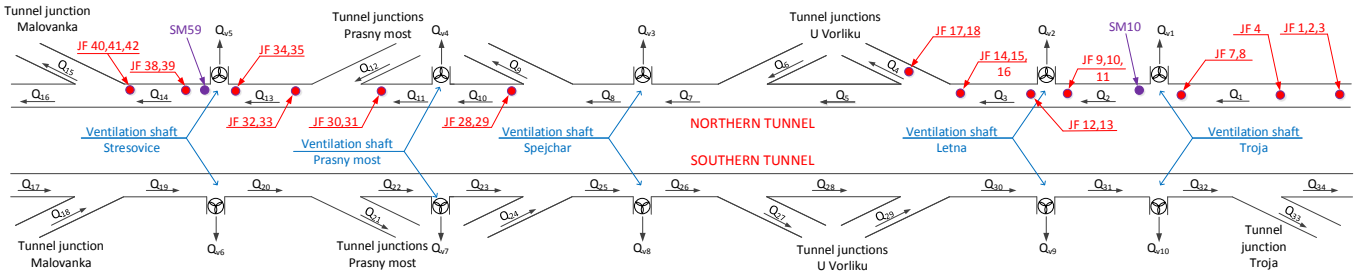

Figure 8: Segmental scheme of the tunnel complex Blanka, including entrance and exit ramps, location of selected jet fans (JF) and ventilation machine rooms (shafts).

The example below gives the set of Bernoulli and continuity equations for the northern tube of the tunnel complex. Recall here that the local acceleration is $a = \frac{\mathrm{d}v}{\mathrm{d}t}$ and that $Q = A \cdot v$.

$$
\begin{aligned}
\rho(L_1a_1 + L_2a_2 + L_3a_3 + L_4a_4) &= \Delta p_1 + \Delta p_2 + \Delta p_3 + \Delta p_4 \\
\rho(L_4a_4 - L_5a_5 + L_6a_6) &= \Delta p_4 - \Delta p_5 + \Delta p_6 \\
\rho(L_6a_6 + L_7a_7 + L_8a_8 + L_9a_9) &= \Delta p_6 + \Delta p_7 + \Delta p_8 + \Delta p_9 \\
\rho(L_9a_9 - L_{10}a_{10} - L_{11}a_{11} + L_{12}a_{12}) &= \Delta p_9 - \Delta p_{10} - \Delta p_{11} + \Delta p_{12} \\
\rho(L_{12}a_{12} + L_{13}a_{13} + L_{14}a_{14} + L_{15}a_{15}) &= \Delta p_{12} + \Delta p_{13} + \Delta p_{14} + \Delta p_{15} \\
\rho(L_{15}a_{15} - L_{16}a_{16}) &= \Delta p_{15} - \Delta p_{16} \\
Q_1 - Q_{v1} - Q_2 &= 0 \\
Q_2 - Q_{v2} - Q_3 &= 0 \\
Q_3 - Q_4 - Q_5 &= 0 \\
Q_5 + Q_6 - Q_7 &= 0 \\
Q_7 - Q_{v3} - Q_8 &= 0 \\
Q_8 - Q_9 - Q_{10} &= 0 \\
Q_{10} - Q_{v4} - Q_{11} &= 0 \\
Q_{11} + Q_{12} - Q_{13} &= 0 \\
Q_{13} - Q_{v5} - Q_{14} &= 0 \\
Q_{14} - Q_{15} - Q_{16} &= 0
\end{aligned}
$$

Here $Q_{v1}, Q_{v2}, \ldots Q_{v10}$ represent the extracted amount of air through ventilation machine rooms.

This can be rewritten in a standard state-space form:

$$\frac{\mathrm{d}\mathbf{v}}{\mathrm{d}t} = f(\mathbf{v}, \mathbf{u}, \mathbf{d}) \tag{17}$$

where $\mathbf{v} \in \mathbb{R}^n$ is the vector of state variables, which is formed by the airflow velocity in each section, $\mathbf{u} \in \mathbb{R}^m$ is the vector of manipulated variables, which are the number of jet fans running in the given section and $\mathbf{d} \in \mathbb{R}^p$ is the disturbance. f is the nonlinear vector field depending on state variables $\mathbf{v}$, system inputs $\mathbf{u}$ and disturbance variables $\mathbf{d}$.

5. Procedure of SIMC tuning method

5.1. Linear model

Once the nonlinear mathematical model is obtained, one can linearize it and design the PI controller for each section of the tunnel using the SIMC method. The linearized model is approximated as a first-order plus time delay model

$$g(s) = \frac{\Delta y}{\Delta u} = \frac{K}{\tau_1 s + 1} \cdot \mathrm{e}^{-\theta s} \tag{18}$$

where Δy is the deviation in airflow velocity from its nominal steady-state value y_p, Δu is the deviation in the manipulated variable from its nominal steady-state value u_p, K is the process gain, τ_1 is the process dominant time constant and θ is the effective time delay.

The simplest approach for obtaining the linear model is to use a step response [9]. The procedure of obtaining these parameters is illustrated in Figure 9, where the system gain K of the model can be calculated as the ratio of the steady-state change in the controlled output and the manipulated variable

$$K = \frac{\Delta y(\infty)}{\Delta u(\infty)} \tag{19}$$

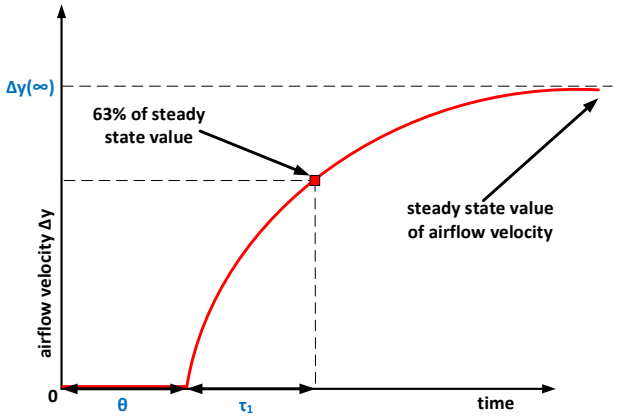

Figure 9: Obtaining the parameters of the linearized model from the step response of the original nonlinear model.

5.2. Controller tuning

The SIMC procedure can be summarized in two steps [9]:

1. Obtain a linear model of the process dynamics in the form (18)
2. Select the parameters of the PI controller (1) as follows:

$$K_c = \frac{1}{K}\frac{\tau_1}{\tau_c + \theta} \tag{20}$$

$$\tau_I = \min\{\tau_1, 4(\tau_c + \theta)\} \tag{21}$$

where τ_c is an adjustable tuning parameter. It is recommended to choose $\tau_c \geq \theta$.

The tuning parameter τ_c is used to get the appropriate trade-off between performance („tight" control with a small τ_c) and robustness („smooth" control with a large τ_c). It is recommended to use $\tau_c = \theta$ as a default value for tight tuning [22].

Grimholt and Skogestad [22] show that there is a linear relationship between the gain margin (GM) and τ_c for processes with a relatively small value of τ_1 (such that the SIMC-rule gives $\tau_I = \tau_1$):

$$GM = \frac{\pi}{2}\left(\frac{\tau_c}{\theta} + 1\right) \tag{22}$$

Thus, a large value of τ_c gives a large GM. Similar simple formulas can be derived for the delay margin ($DM = \Delta\theta/\theta$), which represents the maximum extra time delay to preserve stability:

$$DM = GM - 1 \tag{23}$$

and phase margin (PM):

$$PM = \frac{\pi}{2} - \frac{\theta}{\tau_c + \theta} \tag{24}$$

These simple formulas depend only on the tuning parameter τ_c. With $\tau_c = \theta$ („tight" control), we get $GM = \pi = 3.14$, $DM = 2.14$ and $PM = 61.4°$. For processes where the SIMC-rules give $\tau_I = 4(\tau_c + \theta)$, the margins are slightly worse, but for $\tau_c = \theta$ always better than $GM = 2.96$, $DM = 1.59$ and $PM = 46.9°$ [9]. This is much better than the typical minimum requirements $GM > 1.7$ and $PM > 30°$ [23].

5.3. Choice of operating point for controller tuning

For each detection section, we have a SIMO controller. However, since the adjustment of the manipulated variable is always done using jet fan u_1 (with variable speed drive), it is enough to consider tuning a PI controller with the input u_1 (manipulated variable=relative speed of jet fan 1) and output y (control variable=airflow velocity). The start up of the other jet fans may be considered to be disturbances, as they do not directly affect the closed-loop stability and the performance of the airflow velocity control.

The process from u_1 to y is nonlinear, meaning that the dynamic response will depend on the operating point, for example, on the number of other jet fans in use. In general, a nonlinear process should use a nonlinear controller, but to simplify, we here use a single linear PI controller. To maintain robustness, we should in particular avoid that the controller gain K_c is too large. We use the SIMC-rules for tuning and with the choice $\tau_c = (F-1)\cdot\theta$ (where in general $F \geq 2$ and a large value for F gives more robustness) we have the relationship for the controller gain

$$K_c = \frac{1}{F}\frac{\tau_1}{K\theta} \tag{25}$$

From this we note that a large value of the factor $\frac{\tau_1}{K\cdot\theta}$ gives a large controller gain. Thus, to be robust we should base the controller on an operating point where $\frac{K\cdot\theta}{\tau_1}$ is largest. Since the factor $\frac{K\cdot\theta}{\tau_1}$ generally decreases as we start up more jet fans (see Figure 10 and Tables 2-4 below), this corresponds to the operating point where only jet fan 1 (with the variable speed drive) is operating. For details on the PI controller tuning see sections 6.1 and 6.2.

6. Tuning of the PI controller for the selected sections

In this section, we tune the PI controllers for detection sections SM10 and SM59 (See Figure 8) based on the SIMC-procedure described in 5.1. Section SM59 is located in the Brusnice tunnel near the exit portal Malovanka. In case of fire, smoke is extracted through exit portals and the ventilation machine rooms are not in operation. Section SM10 is located in the Bubeneč tunnel. In case of fire, smoke is extracted through the ventilation machine rooms, which acts as a disturbance for the PI controller.

6.1. Section SM59 without smoke extraction

The priority list for starting the jet fans for section SM59 in the first stage of fire ventilation is:

$$SM59_1 = [34, 28, 35, 33, 32, 31, 30, 29]$$

and in the second stage:

$$SM59_2 = [SM59_1, 41, 42, 40, 39, 38]$$

The location of the jet fans is depicted in Figure 8. In this case, u_1 corresponds to jet fan 34, u_2 to 28, u_3 to 35 etc. The manipulated variable u is distributed by the splitter to jet fans u_{1-8} in the first stage and to u_{1-13} in the second stage.

Note that only jet fans 34, 28 and 41 are equipped with variable speed drive, which allow for a continuous regulation of speed. Although jet fan 41 is equipped with variable speed drive, it is located downstream of the fire, and therefore it can only be used only in the second stage of fire ventilation.

The adjustment of the manipulated variable u is done using u_1 and the start-up of other jet fans $u_2, u_3, \ldots$ acts as a disturbance for the controller. In Figure 10 we show the airflow velocity as a result of the gradual start-up of jet fans (Δu) in section SM59 based on the priority list for the first stage. The simulation is performed for the nonlinear model introduced in Section 4.

As can be seen, the increase of airflow velocity is smaller with every next running jet fan. This behaviour is expected, since the pressure losses increase with the square value of airflow velocity, see Equation (7). Moreover, jet fans 28, 29, 30 and 31 (u_2, u_8, u_7, u_6) have very low influence on airflow velocity, because they are located far from the detection section SM59.

We have also simulated in Figure 11 the effect of $\Delta u_1 = 1$ for different number of other fans running. The blue line shows Δy for $\Delta u_1 = 1$ with no other running jet fans. The red line shows Δy when u_2 (jet fan 28) is running and the green line when also u_3 (jet fan 35) is running. As can be seen, the

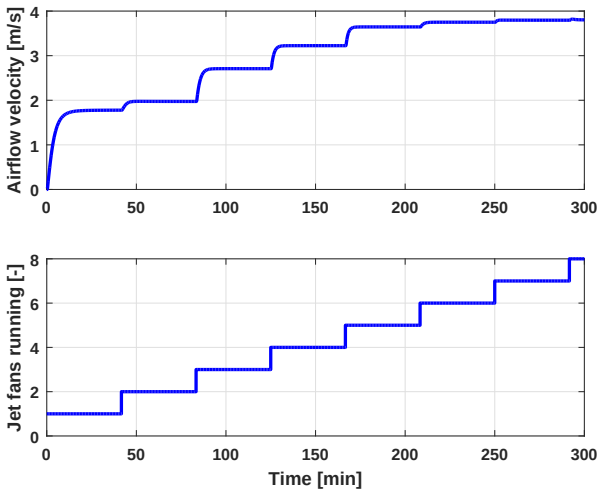

Figure 10: Influence of running jet fans on airflow velocity. The influence of each additional jet fan decreases with the increasing airflow velocity. The simulation is performed for the nonlinear model.

largest process gain K and the largest process slope $K\theta/\tau_1$ is for the blue line, with no other jet fans running. This can also be seen from Tables 2-4, which summarize the linearized models for the same cases.

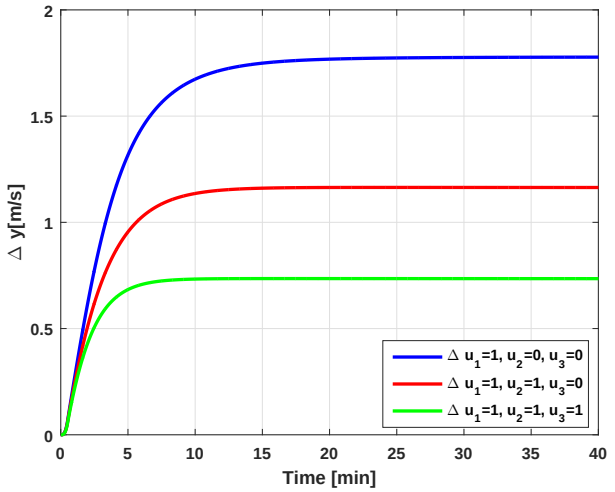

Figure 11: Influence of u_1 (jet fan 34) on the airflow velocity in the tunnel with simultaneous operation of other jet fans.

We must find an operating point for the system linearization. We have argued in Section 5.3 that the best choice is the operating point where only u_1 (jet fan 34) operates. We therefore choose the case $\Delta u_1 = 1$ and use the following linearized model for the design of the PI controller in section SM59:

$$g_1(s) = \frac{1.78}{213s + 1} \cdot \mathrm{e}^{-20s} \tag{26}$$

The PI controller was tuned using SIMC-formulas (20) and (21). The tuning parameter τ_c should be chosen in order to fulfil

Table 2: Parameters of linearized models for different values of Δu_1 with no other jet fans running.

$u_2 = 0, u_3 = 0$	K	τ_1	θ	$\frac{K\theta}{\tau_1}$
$\Delta u_1 = 0.3$	1.72	648	33	0.09
$\Delta u_1 = 0.5$	1.76	411	20	0.09
$\Delta u_1 = 0.7$	1.77	297	20	0.12
$\mathbf{\Delta u_1 = 1}$ (Fig. 11)	**1.78**	**213**	**20**	**0.17**

Table 3: Parameters of linearized models for different values of Δu_1 with u_2 running simultaneously.

$u_2 = 1, u_3 = 0$	K	τ_1	θ	$\frac{K\theta}{\tau_1}$
$\Delta u_1 = 0.3$	0.42	223	14	0.03
$\Delta u_1 = 0.5$	0.69	212	13	0.04
$\Delta u_1 = 0.7$	0.91	196	13	0.06
$\Delta u_1 = 1$ (Fig. 11)	1.16	175	13	0.09

Table 4: Parameters of linearized models for different values of Δu_1 with u_2 and u_3 running simultaneously.

$u_2 = 1, u_3 = 1$	K	τ_1	θ	$\frac{K\theta}{\tau_1}$
$\Delta u_1 = 0.3$	0.22	137	12	0.02
$\Delta u_1 = 0.5$	0.40	140	12	0.03
$\Delta u_1 = 0.7$	0.56	133	12	0.05
$\Delta u_1 = 1$ (Fig. 11)	0.73	121	12	0.07

the requirements on airflow velocity control, stated in Section 2.2. The PI controller was tuned for several values of τ_c,

$$\tau_c = \theta/2, \quad \tau_c = \theta, \quad \tau_c = 2\theta, \quad \tau_c = 4\theta.$$

to show how different results we achieve with different τ_c. The corresponding settings of the PI-controllers are given in Table 5. The table also includes gain margin (GM), delay margin ($DM = \Delta\theta/\theta$) and phase margin (PM).

Table 5: SIMC PI-controllers for different values of τ_c for section SM59 for model (26) with $\theta = 20$ s.

τ_c	K_c	τ_I	GM	$\Delta\theta/\theta$	PM
$\theta/2$	4	120	2.28	1.16	45.13°
θ	3	160	3.10	1.99	57.63°
2θ	2	213	4.71	3.71	70.90°
4θ	1.2	213	7.85	6.85	78.54°

The corresponding responses using the nonlinear model are shown in Figure 12. Both stages of fire ventilation were simulated, and the second stage starts after 10 minutes of simulation. Section SM59 has the following airflow velocity set-point settings for the two stages:

$$y_{sp1} = 1.6\,\mathrm{m/s}, \quad y_{sp2} = 3.4\,\mathrm{m/s}$$

The PI-simulations include all limitations described in Section 3.5, including saturation, anti wind-up protection and limitations for jet fans equipped with variable speed drive.

As can be seen from Fig. 12, the PI controller tuned with $\tau_c = \theta$ fulfills the requirements on airflow velocity control; the

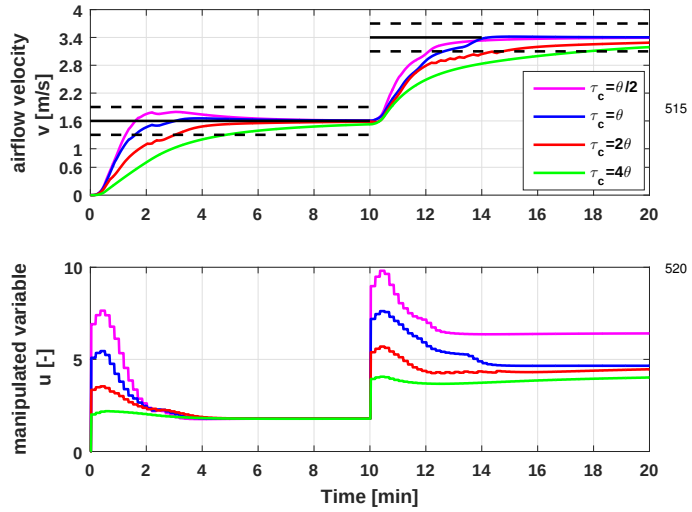

Figure 12: Nonlinear simulation of section SM59 with PI controller tuned with different parameters τ_c. Simulation was performed using nonlinear model. The black line represents airflow set-point value and the dashed black line the allowed range of variation (± 0.3 m/s from set-point).

allowed range of airflow velocity (± 0.3 m/s from the set-point value) is achieved within 3 minutes and the airflow velocity is kept within this range. Also the PI controller with $\tau_c = \theta/2$ fulfills these requirements, but it is more aggressive and does not improve performance too much.

Therefore, for real operation, we recommend to use a PI controller with $\tau_c = \theta$ and the following settings

$$K_c = 3, \quad \tau_I = 160.$$

Moreover, with $\tau_c = \theta$, we get a robust design with $GM = 3.10$, $\Delta\theta/\theta = 1.99$ and $PM = 57.63°$.

6.2. Section SM10 with smoke extraction

The control of the longitudinal airflow velocity in section SM10 is more challenging than in section SM59, since the ventilation machine rooms for smoke extraction are in operation. There are two ventilation machine rooms, Letná and Troja, which run simultaneously during the fire ventilation. The start-up of the ventilation machine rooms for smoke extraction has a large influence on airflow velocity and acts as a disturbance for the control system.

The priority list for jet fans start-up in the first stage of fire ventilation is:

$$SM10_1 = [7, 4, 8, 3, 2, 1]$$

and in the second stage:

$$SM10_2 = [SM10_1, 18, 15, 10, 17, 16, 14, 13, 12, 11, 9]$$

Here u_1 corresponds to jet fan 7, u_2 to jet fan 4, etc. The location of jet fans in section SM10 is shown in Fig. 8. Six jet fans are available for control in the first stage of fire ventilation and jet fans 7 and 4 (for both first and second stage) and 18 and 15 (only for second stage) are equipped with variable speed drive.

The airflow velocity set-points for two stages are:

$$y_{sp1} = 0.9\,\mathrm{m/s}, \quad y_{sp2} = 1.9\,\mathrm{m/s}$$

The SIMC-procedure for the design of the PI controller is the same as for section SM59. Tables 6, 7 and 8 give the parameters of the linearized models for different values of Δu_1 for $u_2 = u_3 = 0$ (Table 6), $u_2 = 1, u_3 = 0$ (Table 7) and $u_2 = u_3 = 1$ (Table 8). Again, the largest value of $\frac{K\theta}{\tau_1}$ is used to find the linearized model for the design of the PI controller.

Table 6: Parameters of linearized models for different values of Δu_1. No other jet fans running.

$u_2 = 0, u_3 = 0$	K	τ_1	θ	$\frac{K\theta}{\tau_1}$
$\Delta u_1 = 0.3$	1.29	853	43	0.06
$\Delta u_1 = 0.5$	1.34	546	24	0.06
$\Delta u_1 = 0.7$	1.34	393	22	0.07
$\mathbf{\Delta u_1 = 1}$	**1.34**	**279**	**22**	**0.11**

Table 7: Parameters of linearized models for different values of Δu_1. u_2 running simultaneously.

$u_2 = 1, u_3 = 0$	K	τ_1	θ	$\frac{K\theta}{\tau_1}$
$\Delta u_1 = 0.3$	0.21	218	14	0.03
$\Delta u_1 = 0.5$	0.36	209	13	0.04
$\Delta u_1 = 0.7$	0.48	196	13	0.06
$\Delta u_1 = 1$	0.63	176	13	0.09

Table 8: Parameters of linearized models for different values of Δu_1. u_2 and u_3 running simultaneously.

$u_2 = 1, u_3 = 1$	K	τ_1	θ	$\frac{K\theta}{\tau_1}$
$\Delta u_1 = 0.3$	0.12	141	12	0.01
$\Delta u_1 = 0.5$	0.22	140	12	0.02
$\Delta u_1 = 0.7$	0.31	138	12	0.03
$\Delta u_1 = 1$	0.44	134	12	0.04

The ratio $\frac{K\theta}{\tau_1}$ is highest for the change $\Delta u_1 = 1$ with no other running jet fans ($u_2 = u_3 = 0$). Hence, we choose the following linearized model for the design of the PI controller:

$$g_2(s) = \frac{1.34}{279s + 1} \cdot \mathrm{e}^{-22s} \tag{27}$$

The PI controllers were tuned for different values of τ_c and the PI-parameters are given in Tab. 9.

Table 9: SIMC PI-controllers for different values of τ_c in section SM10 for the model (27) with $\theta = 22$ s.

τ_c	K_c	τ_I	GM	$\Delta\theta/\theta$	PM
$\theta/2$	6.32	132	2.26	1.12	43.8°
θ	4.74	176	3.08	1.92	55.85°
2θ	3.16	264	4.70	3.66	70.12°
4θ	1.89	279	7.85	6.85	78.54°

The corresponding nonlinear closed-loop simulations are shown in Fig. 13. In this case, all these controllers fulfill the requirements on the airflow velocity control, because the allowed range of airflow velocity is achieved within 3 minutes.

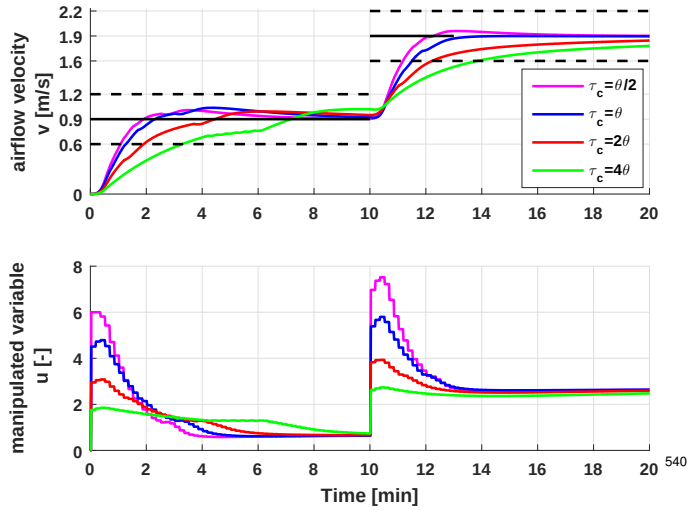

Figure 13: Nonlinear simulation of section SM10 with PI controller tuned with different values of τ_c for section SM10. The black line represents the set-point and dashed black line allowed range of the airflow velocity.

Effect of disturbance from ventilation machine rooms

The simulation in Fig. 14 includes a disturbance in the airflow extraction with the extraction capacity of $Q_{vm} = 220\ \mathrm{m}^3/\mathrm{s}$ in the first stage and $Q_{vm} = 312\ \mathrm{m}^3/\mathrm{s}$ in the second stage. The second stage starts 15 minutes after the beginning of the simulation. As can be seen, the start-up of the ventilation machine rooms causes an increase of airflow velocity and there is an overshoot in the airflow velocity initially. However, all controllers are able to suppress the disturbance after a few minutes. We recommend to use the controller with $\tau_c = \theta$ for the real operation, since it results in a good trade-off between performance and robustness among all simulated controllers. This controller has the following parameters

$$K_c = 4.74, \quad \tau_I = 176\ \mathrm{s}.$$

With this controller, we obtain a robust design with $GM = 3.08$, $\Delta\theta/\theta = 1.92$ and $PM = 55.85°$.

7. Comparing simulations with real data

This section compares simulations with real measured data obtained from tunnel testing before opening of the tunnel. The real discrete-time PI controllers were tuned using the root locus method with sample time $\Delta T = 10$ s. Note that the design of the PI controllers using the SIMC method was performed after the opening of the Blanka tunnel complex, but the resulting tuning are actually quite similar.

It is necessary to mention that the simulation and real measured data can never be compared under the same conditions.

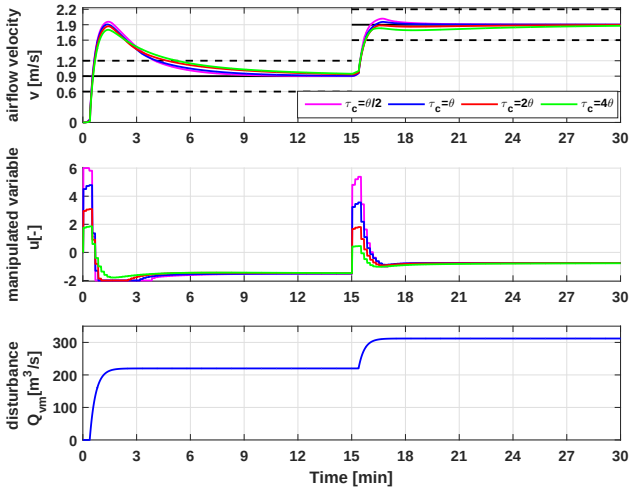

Figure 14: Nonlinear simulation of section SM10, which also include a disturbance Q_{vm} caused by start-up of the ventilation machine rooms.

The airflow velocity in the tunnel is strongly influenced by the location of the jet fans, see Fig. 10. Jet fans with soft-starters are activated during the simulations and as stated in Section 3.1, jet fans equipped with soft-starters have at most 6 starts per hour and there is a minimum time of 6 minutes before each stop and start. During this time, these jet fans are not available for the control system. Moreover, some failures of jet fans caused by electrical protection occurred during the real testing. Thus, it is not guaranteed that the splitter activates the same jet fans in simulation and real operation. Unfortunately, we did not log the exact activation of jet fans during the real tests.

7.1. Section SM59 without smoke extraction

First we compare simulations and real data for section SM59. The real PI controller tuned using the root locus method has the following parameters for the first stage:

$$K_c = 3, \quad \tau_I = 100\ \mathrm{s}, \quad K_c/\tau_I = 0.03$$

and for the second stage:

$$K_c = 2, \quad \tau_I = 100\ \mathrm{s}, \quad K_c/\tau_I = 0.02.$$

To compare, the controller tuned by SIMC has the following constants for both stages of fire ventilation:

$$K_c = 3, \quad \tau_I = 160\ \mathrm{s}, \quad K_c/\tau_I = 0.018.$$

The result of the comparison is shown in Figure 15. There are three lines; the real measured data (red), the simulation with the PI controller tuned by the root locus method (blue) and the simulation with the SIMC PI controller (green). We see that the second stage starts after approximately 11.5 minutes.

Both PI-controllers (root locus and SIMC) achieve the allowed range of airflow velocity within 3 minutes and the airflow velocity is kept within this range. The SIMC PI controller is slightly slower than the root locus PI controller in the first stage, but it is more robust due to the larger integral time constant. If

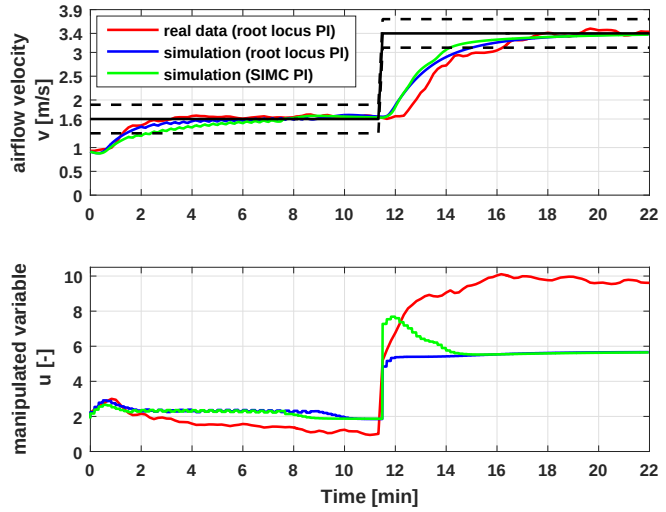

Figure 15: Comparison of real data with simulation in section SM59.

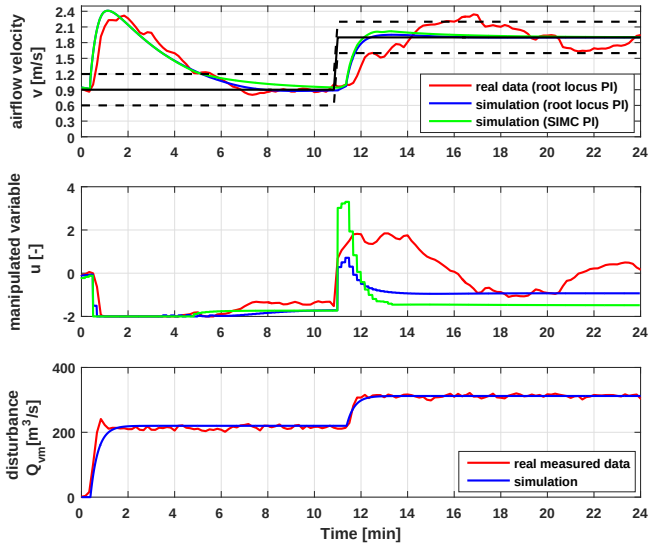

Figure 16: Comparison of real data with simulation for section SM10.

needed, the SIMC PI controller can be tuned with smaller value of τ_c for the faster response, but with less robustness.

As can be seen, there are some deviations between the real measured data (red line) and the simulation data (blue line), especially in the second stage of fire ventilation, where the real time delay is slightly larger. These deviations can be caused by differently activated jet fans. Further, we neglected the stack effect caused by temperature difference of tunnel portals and also the wind effect at tunnel portals. Moreover, during the tunnel testing, there were vehicles passing through the tunnel, which influenced the airflow velocity.

If one takes these facts into account and also notice that the nonlinear model was obtained based only on physical principles (white-box model) and not on real measured data, then the model compares very satisfactorily with reality.

Although the steady state values of airflow velocity v are same for the blue and red line, the steady state values of the manipulated variable u are different in the second stage of fire ventilation. This is because of the quadratic dependence of pressure losses on airflow velocity, see Equation (7), which gives a lower model gain with increasing airflow velocity. In other words, there is almost no difference with 6 or 10 activated jet fans, see Fig. 10.

An important result of this simulation is that it is not necessary to have different settings for the PI controller in the two stages of fire ventilation.

7.2. Section SM10 with smoke extraction

The real PI controller tuned via the root locus method has the same setting for both phases of fire ventilation:

$$K_c = 2, \quad \tau_I = 66.67\,\text{s}, \quad K_c/\tau_I = 0.03.$$

To compare, the PI controller tuned with SIMC has the following setting

$$K_c = 4.74, \quad \tau_I = 176\,\text{s}, \quad K_c/\tau_I = 0.027.$$

Note that the value of K_c/τ_I is similar for the two controllers.

The comparison of simulation with real data is shown in Fig. 16. The ventilation control test consists of two stages, where the second stage starts at around 11 minutes. The ventilation machine rooms Letná and Troja are in operation in this case and the extraction capacity was set to 220 m^3/s in the first stage and 312 m^3/s in the second stage. As can be seen in the upper airflow velocity graph, the root locus method (blue line), again, is similar to the SIMC method (green line). Both controllers suppress the disturbance caused at start-up of the ventilation machine rooms and both keep the airflow velocity in the allowed range.

Although the SIMC PI controller starts more redundant jet fans in the beginning of the second stage due to the higher K_c, we prefer a slightly faster SIMC PI (for $\tau_c = \theta$) to ensure the good performance under unfavorable conditions in the tunnel. In some cases, the airflow velocity control can start with the negative airflow velocity, and thus the direction of airflow must be turned as fast as possible.

Again, the simulation (blue line) shows a fairly good agreement with the reality (red line) in the first stage of fire ventilation control. There are some discrepancies between the simulation and reality in the second stage. These discrepancies can be caused by ventilation machine rooms, which extract the air from the tunnel. The effect of air extraction is simply modeled via mass balance equation in our simulation model and pressure losses in ventilation machine rooms are neglected, because they cannot be simply modeled in the 1D model.

8. Conclusion

This paper presents a systematic approach for the design of PI controllers for fire ventilation in road tunnels using the SIMC procedure. As a case study we consider the Blanka tunnel complex in Prague, Czech Republic. The agreement between real

data and nonlinear simulations based on a first-principle model is very good. The results indicate that the SIMC procedure is very suitable, especially, if a nonlinear model of the process dynamics is available. In summary, the SIMC tuning method can be used for the design of controllers in future road tunnels, especially in complex road tunnels, where the tuning can be time consuming.

Acknowledgements

This work has been developed during the first author's internship at the Norwegian University of Science and Technology (NTNU), which has been supported by Norway grants within the programme CZ07. This work has been further supported by the University Centre for Energy Efficient Buildings of Technical University in Prague and through the internal grant of CTU SGS16/232/OHK3/3T/13. Many thanks go to Heinz Preisig from NTNU and to the ventilation designers of the Blanka tunnel complex; Jiří Zápařka and Jan Pořízek from the company Satra, s.r.o., Jiří Cigler from the company Feramat Cybernetics, s.r.o. and Lukáš Ferkl from CTU in Prague, since their valuable advices and comments contributed to the final version of this paper.

References

[1] P. Sturm, M. Beyer, M. Rafiei, On the problem of ventilation control in case of a tunnel fire event, Case Studies in Fire Safety doi:10.1016/j.csfs.2015.11.001.
URL http://www.sciencedirect.com/science/article/pii/S2214398X15300030

[2] PIARC, Road tunnels manual - 2.Safety, Tech. rep. (2011).

[3] PIARC, Road Tunnels: Operational Strategies for Emergency Ventilation, PIARC Technical Committee 3.3 Road Tunnel Operation (2011).

[4] I. Espinosa, S. Fernández, I. Del Ray, E. Alarcón, Experiences on the Specification of Algorithms for Fire and Smoke Control in Road Tunnels.pdf, in: Proceedins of the 5th International Conference - Tunnel Safety and Ventilation, Graz, 2010, pp. 39–43.

[5] P. Pospisil, R. Brandt, Smoke control in road tunnels, in: Proceedings of the Conference Significance of Tunnels in Transport, Podbanské (Slowakia), 2005, pp. 1–6.

[6] N. Euler-Rolle, M. Fuhrmann, M. Reinwald, S. Jakubek, Longitudinal tunnel ventilation control. part 1: Modelling and dynamic feedforward control, Control Engineering Practice 63 (2017) 91 – 103. doi:http://dx.doi.org/10.1016/j.conengprac.2017.03.017.
URL http://www.sciencedirect.com/science/article/pii/S0967066117300758

[7] A. Visioli, Advances in Industrial Control, part Practiacal PID Control, 2011. doi:10.1007/978-1-4471-4399-4.
URL http://www.springer.com/engineering/control/book/978-0-85729-634-4

[8] D. Rivera, M. Morari, S. Skogestad, Internal model control: PID controller design, Industrial & Engineering Chemistry Process Design and Development 25 (1986) 252–265. doi:10.1021/i200032a041.
URL http://pubs.acs.org/doi/abs/10.1021/i200032a041

[9] S. Skogestad, Simple analytic rules for model reduction and PID controller tuning, Journal of Process Control 13 (2003) 291–309. doi:10.1016/S0959-1524(02)00062-8.

[10] Satra s.r.o., About the Blanka tunnel complex (2016).
URL http://www.satra.cz/en/blanka-tunnel-complex/

[11] Satra s.r.o., Databank of the company.

[12] J. Karlíček, Tunelový komplex Blanka (2016).
URL http://jakubkarlicek.cz/portfolio/tunelovy-komplex-blanka/

[13] J. Šulc, L. Ferkl, J. Cigler, J. Zápařka, Model-based airflow controller design for fire ventilation in road tunnels, Tunnelling and Underground Space Technology 60 (2016) 121–134. doi:10.1016/j.tust.2016.08.006.

[14] P. Pospisil, METODICKÝ POKYN – Větrání silničních tunelů. Volba systému, navrhování, provoz a zabezpečení jakosti větracích systémů silničních tunelů (in Czech), Tech. rep. (2013).

[15] D. Dimitris, W. Rider, High-Resolution Methods for Incompressible and Low-Speed Flows, Vol. 1, Springer, 2005. doi:10.1007/b137615.

[16] P. K. Kundu, I. M. Cohen, D. R. Dowling, Fluid Mechanics, Elsevier, 2016. doi:10.1016/B978-0-12-405935-1.18001-3.
URL http://www.sciencedirect.com/science/article/pii/B9780124059351180013

[17] CETU, Dossier pilote des tunnels equipements, section 4.1, Ventilation, Tech. rep. (2003).

[18] K. Opstad, P. Aune, J. Henning, Fire emergency ventilation capacity for road tunnels with considerable slope, in: Proceedings of the 9th International Symposium on Aerodynamics and Ventilation of Vehicle Tunnels, Aosta, 1997, pp. 535–543.

[19] H. Ingason, A. Lönnermark, Y. Z. Li, Model of ventilation flows during large tunnel fires, Tunnelling and Underground Space Technology 30 (2012) 64 – 73. doi:http://dx.doi.org/10.1016/j.tust.2012.02.007.
URL http://www.sciencedirect.com/science/article/pii/S0886779812000399

[20] B. Dally, Woods Practical Guide To Fan Engineering, Woods of Colchester Limited, 1992.

[21] P. Frauenfelder, Introduction to Physics: Mechanics, Hydrodynamics, Thermodynamics, Pergamon, 1966.

[22] C. Grimholt, S. Skogestad, Optimal PI-Control and Verification of the SIMC Tuning Rule, in: Proceedings of the 2nd IFAC Conference on Advances in PID Control, Brescia, 2012, pp. 11–22.

[23] D. E. Seborg, D. A. Mellichamp, T. F. Edgar, F. J. Doyle, Process Dynamics and Control, Wiley, New York, 1989.